

# Development of Charge Distribution Measurement System using Pockels Effect

Masayasu ISHIKAWA, Hiroko SAITO, Yasuhiro TANAKA, Yoshihiro MUROOKA, Tatsuo TAKADA and Nobuyuki TOMITA

Electronic Measurement Laboratory, Musashi Institute of Technology

1-28-1 Tamazutsumi, Setagaya-ku, Tokyo 158-8557, Japan

Tel +81-3-3703-3111 (3932) Fax +81-3-5707-2156 E-mail ishikawa@me.musashi-tech.ac.jp

## ABSTRACT

A new system for charge distribution measurement in bulk of dielectrics has been developed. It is important to study the mechanism of charging and discharging process of insulating materials under cosmic rays. Therefore, we have been tried to develop the new system of charge distribution measurement system using Pockels effect. When the polarized laser light is passed through the Pockels crystal, which has electric field distribution, the penetrated light has phase retardation. By detecting the intensity of the light through an analyzer, the electric field can be calculated. As a first attempt, in this paper, we would like to show the results of two-dimensional uniform electric field distributions obtained by measuring the Pockels crystal after corona discharge on its surface. These results show that this technique is available to the monitoring system of cosmic rays for the spacecraft

## INTRODUCTION

In general, it is well known that spacecraft flying in the higher altitude such as GEO orbit is exposed to the high-energy cosmic rays, then the insulating materials of spacecraft is charged up. The discharge following the charging up of the insulating materials of spacecraft cause the degradation of materials and sometimes give a damage to electronics on-board. Therefore, it is required to analyze the mechanism of charge accumulation in bulk of insulating materials in actual space environment [1].

From this viewpoint, we are attempting to develop the monitoring system for high-energy charged particles using electro-optic Pockels effect. The new monitoring system has an advantage of measuring the charge distribution in the dielectric material as shown in Table 1. The energy level of charged particles

penetrated into the material can be evaluated from the penetrated depth of charged particles  $\Delta y(x,y)$  corresponding to the phase retardation distribution  $\Delta\theta_s(x,y)$ . Furthermore, the amount of charged particles can be also estimated using measured value of the phase retardation  $\Delta\theta_s(x,y)$ . In this paper, the relationship between  $\Delta y(x,y)$  and  $\Delta\theta_s(x,y)$  will be analytically mentioned, then experimentally obtained results will be introduced.

## FUNDAMENTALS FOR ELECTRO-OPTIC POCKELS EFFECT

The possibility for monitoring cosmic rays using a LiNbO<sub>3</sub> crystal, which exhibits the electro-optical Pockels effect, is proposed here. When the LiNbO<sub>3</sub> crystal is irradiated with cosmic rays, the accumulated charges build up a distorted electric field distribution  $E(x,y,z)$ , and modify the optical properties of the crystal via the Pockels effect. Even for a linearly polarized incident light, an additional optical retardation distribution  $\Delta\theta_s(x,y)$  yields between the two perpendicular components of electrical field of the transmitted light. For an incident light propagating along the z axis, i.e., the optical axis of the LiNbO<sub>3</sub> crystal, the resultant retardation distribution  $\Delta\theta_s(x,y)$  depends on both components,  $E_x(x,y)$  and  $E_y(x,y)$ , of the internal electrical field  $E(x,y,z)$  perpendicular to the light propagation direction. In this case, the retardation distribution  $\Delta\theta_s(x,y)$  allows for measurement of these two field components of  $E_x(x,y)$  and  $E_y(x,y)$ . On the other hand, for an incident light propagating along the direction perpendicular to the optical axis, the resultant retardation distribution  $\Delta\theta_s(x,y)$  depends also on the field component of  $E_z(x,y)$ . In this case,  $\Delta\theta_s(x,y)$  allows for measurement of the  $E_z(x,y)$  field component. In the following explanation, only the former case will be discussed.

Table 1. Characteristics of new monitoring system for high energy charged particles using electro-optic Pockels effect.

Cosmic ray		Radiation energy	Amount of dose
High energy charged particles	Electron Negative ion Positive ion	Measurement of penetration depth $\Delta y(x,y)$	Accumulated charge quantity $\Delta K_p(x,y)$
Electromagnetic wave	X-ray (1keV~500keV) Gamma ray (over 1MeV)	Measurement of penetration depth $\Delta y(x,y)$	Accumulated charge quantity $\Delta K_p(x,y)$
Measurement technique: Electro-optic Pockels effect		Distribution of phase retardation $\Delta\theta(x,y)$	Amount of phase retardation $ \Delta\theta(x,y) $

## EFFECTS OF FIELD COMPONENTS

For incident light propagating along the z axis, which is the optical axis of the LiNbO<sub>3</sub> Pockels crystal, the equation describing the effective ellipse of birefringence at the orthogonal x-y plane can be given as shown in following Eq.(1).

$$\left( \frac{1}{n_0^2} - \gamma_{22} E_y + \gamma_{13} E_z \right) x^2 + \left( \frac{1}{n_0^2} + \gamma_{22} E_y + \gamma_{13} E_z \right) y^2 - 4\gamma_{22} E_x xy = 1 \quad (1)$$

Where  $n_0$  is a refractive index for normal light and  $\gamma_{22}$  and  $\gamma_{13}$  are Pockels constants of the crystal. For case (1) when only the  $E_x(x,y)$  field component is considered, Eq.(1) becomes

$$\frac{1}{n_0^2} x^2 + \frac{1}{n_0^2} y^2 - 4\gamma_{22} E_x xy = 1 \quad (2)$$

From this equation (2), it is found that the refractive index at the slow-axis of  $+45^\circ$  increases to  $n_0 + n_0^3 \gamma_{22} E_x$ , while the refractive index at the fast-axis of  $-45^\circ$  decreases to  $n_0 - n_0^3 \gamma_{22} E_x$  as shown in Fig.1(a). For incident light polarized along the x-axis direction, a retardation distribution  $\Delta\theta_{S1}(x,y)$  is produced between the two components of the electric field of the transmitted light. In this case, one of the components is along the slow-axis direction of  $+45^\circ$ , and the other is along the fast-axis direction of  $-45^\circ$ . The retardation  $\Delta\theta_{S1}(x,y)$  is given by

$$\Delta\theta_{S1}(x,y) = \frac{2\pi}{\lambda} 2n_0^3 \gamma_{22} \bar{E}_x(x,y) l \quad (3)$$

where  $\lambda$ ,  $l$  and  $\bar{E}_x(x,y)$  are wave-length of light, optical path length and average of  $E_x(x,y)$  in the crystal along the z direction, respectively.

$E_x(x,y)$  in above equation is given by

$$\bar{E}_x(x,y) = \int_0^l E_x(x,y,z) dz / l \quad (4)$$

For case (2), when only the  $E_y(x,y)$  field component is considered, Eq.(1) becomes

$$\left( \frac{1}{n_0^2} - \gamma_{22} E_y \right) x^2 + \left( \frac{1}{n_0^2} + \gamma_{22} E_y \right) y^2 = 1 \quad (5)$$

It is found that the refractive index at the slow-axis of  $0^\circ$  increases to  $n_0 + n_0^3 \gamma_{22} E_y / 2$ , while the refractive index at the fast-axis of  $+90^\circ$  decreases to  $n_0 - n_0^3 \gamma_{22} E_y / 2$  as shown in Fig.1(b). For the incident light polarized at  $45^\circ$ , a retardation distribution  $\Delta\theta_{S2}(x,y)$  is produced between the two components of the electrical field of the transmitted light. In this case, one of the components is along the slow-axis direction of  $0^\circ$  and the other is along the fast-axis direction of  $90^\circ$ . The retardation  $\Delta\theta_{S2}(x,y)$  is given by

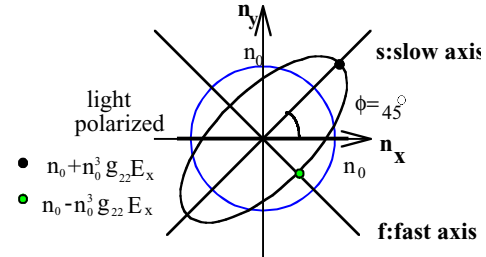
$$\Delta\theta_{S2}(x,y) = \frac{2\pi}{\lambda} n_0^3 \gamma_{22} \bar{E}_y(x,y) l \quad (6)$$

Where  $\bar{E}_y(x,y)$  is the average of  $E_y(x,y)$  in the crystal along the z direction.

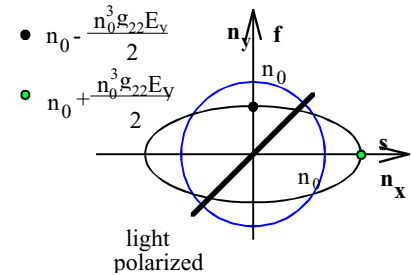
The  $E_y(x,y)$  in above equation is given by

$$\bar{E}_y(x,y) = \int_0^l E_y(x,y,z) dz / l \quad (7)$$

It is interesting that, for case (1) when the incident light is polarized at the angle of  $0^\circ$ , which is the same angle of the slow-axis in case (2), the retardation  $\Delta\theta_S(x,y)$  only depends on field component of  $E_x(x,y)$  and it is independent of  $E_y(x,y)$ . On the other hand, for case (2) when the incident light is polarized at the angle of  $+45^\circ$ , which is the same angle of the slow-axis in case (1), the retardation  $\Delta\theta_S(x,y)$  only depends on the electric field  $E_y(x,y)$  and it is independent of  $E_x(x,y)$ . In either case, only one field component of either  $E_x(x,y)$  or  $E_y(x,y)$  effects on the retardation  $\Delta\theta_S(x,y)$  independently. Therefore only one component of either  $\Delta\theta_{S1}(x,y)$  or  $\Delta\theta_{S2}(x,y)$  is able to be measured by choosing the axis angles of the polarizer and the analyzer.



(a) The effective ellipse of birefringence when electric field are  $E_x=E_x$   $E_y=0$   $E_z=0$



(b) The effective ellipse of birefringence when electric field are  $E_y=E_y$   $E_x=0$   $E_z=0$

Fig.1 The model of the effective ellipse of birefringence at the orthogonal x-y plane.

## MEAN ELECTRICAL FIELD DISTRIBUTION AND MEAN CHARGE DENSITY DISTRIBUTION

When a LiNbO<sub>3</sub> Pockels crystal is irradiated with high-energy charged particles, a volume charge density distribution  $\rho(x,y,z)$  accumulates internally and builds up an internal electric field vector distribution  $E(x,y,z)$ , which is governed by Poisson equation,  $\text{div}E(x,y,z)=\rho(x,y,z)/\epsilon$ , where  $\epsilon$  is a dielectric constant of the Pockels crystal. Such a mathematical relationship can be rewritten as

$$\frac{\partial E_x(x,y,z)}{\partial x} + \frac{\partial E_y(x,y,z)}{\partial y} + \frac{\partial E_z(x,y,z)}{\partial z} = \frac{\rho(x,y,z)}{\epsilon} \quad (8).$$

This equation means that any partial differential,  $\partial E_x(x,y,z)/\partial x$ ,  $\partial E_y(x,y,z)/\partial y$  or  $\partial E_z(x,y,z)/\partial z$ , in any component of the electrical field vector distribution  $E(x,y,z)$  is proportional to the charge distribution  $\rho(x,y,z)$ . The energy level and dose rate of the charged particles are evaluated from scaled charge distribution  $K\rho(x,y)$  as shown in Table 1. Therefore, if the average,  $\bar{E}_x(x,y)$ ,  $\bar{E}_y(x,y)$  or  $\bar{E}_z(x,y)$  of any component of the electrical field vector distribution  $E(x,y,z)$  is measured, we can evaluate both the penetration depth  $\Delta y(x,y)$  and the scaled accumulated charge  $K\rho(x,y)$ , then finally the energy level and dose rate of the charged particles are obtained.

## MEASUREMENT SYSTEM

Figure 2 shows the optical measurement system for observing 2-dimentional birefringence distribution

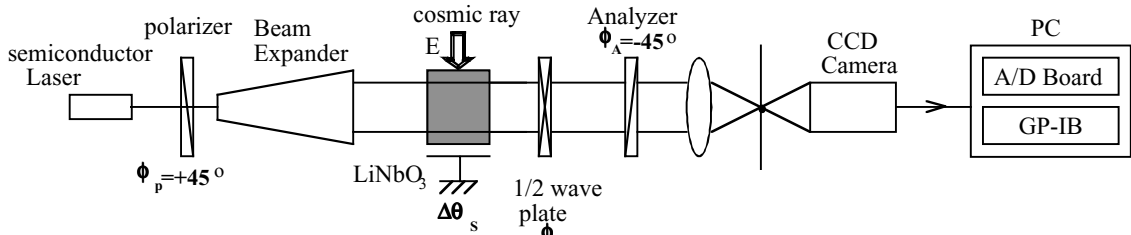


Fig.2 2-Dimensional birefringence measurement system

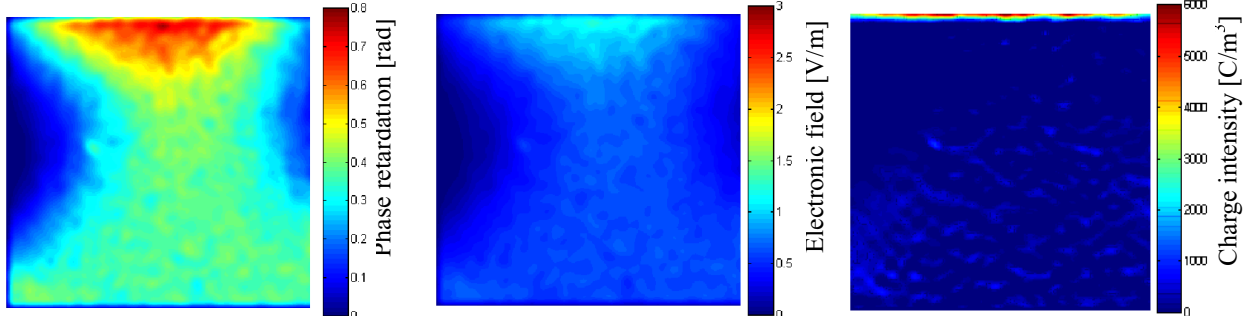


Fig.3 Results of phase retardation distribution, electric field distribution and charge distribution obtained at the condition of positive corona streamer existed on the surface of LiNbO<sub>3</sub> crystal

caused by the electric charges accumulated in the LiNbO<sub>3</sub> Pockels crystal. The system is consisted of semiconductor laser (wave length : 632.8nm), polarizer, beam expander (40mm in diameter), LiNbO<sub>3</sub> Pockels crystal (15x15x15mm<sup>3</sup>), 1/2 wave plate, analyzer, and high sensitive CCD camera. Here, light signals corresponding to  $\Delta\theta_s(x,y)$  are recorded in the CCD camera. Using the beam expander and CCD camera, the digitized image of charge distribution can be obtained with the 2-dimentional light signals. Finally, an electric field distribution in the LiNbO<sub>3</sub> crystal is obtained using the digitized image signals.

## RESULT and DISCUSSION

Figure 3 shows typical results of phase retardation distribution, electric field distribution and charge distribution obtained after negative corona discharge on the surface of LiNbO<sub>3</sub> crystal. Corona is discharged form the needle electrode of 4kV. The needle electrode was put on the surface of LiNbO<sub>3</sub> crystal. Fig.3(a) shows the phase retardation  $\Delta\theta_s(x,y)$  in the LiNbO<sub>3</sub> crystal observed just after corona discharge. Fig.3(b) shows the electric field distribution calculated using result of Fig.3(a). Judging from these figures, it can be seen that the large phase retardation distribution and electric field distribution are located near upper surface of the LiNbO<sub>3</sub>. Fig.3(c) shows the charge distribution in the LiNbO<sub>3</sub>crystal calculated from the result of Fig.3(b). It is hard to find out the charge distribution in the bulk of LiNbO<sub>3</sub> crystal. This mean that the energy level of the corona discharge is too small to penetrate into LiNbO<sub>3</sub> crystal.

## **CONCLUSION**

We succeeded in measuring a 2-dimensinal birefringence distribution generated after corona discharge on LiNbO<sub>3</sub> crystal using the advanced measurement system using electro-optic Pockels effect. Using the measurement result of birefringence distribution, the electric field and charge distributions are calculated. In the case of corona discharge, it is found that the charges are not injected into the bulk of LiNbO<sub>3</sub> crystal. To confirm whether the system is available as the monitoring sensor for high-energy charged particle, it is necessary to measure the birefringence distribution in the bulk of LiNbO<sub>3</sub>, which is irradiated by high-energy charged particles.

## **REFERENCE**

- [1] H.Nishimoto, H.Fujii, and T.Abe, Observation of Surface Charging on Engineering Test Satellite V of Japan , AIAA 27th Aerospace Science Meeting, AIAA-89-0613(1989)
- [2] H.Saito, T.Urabe, Y.Tanaka, T.Takada, and Y.Murooka, Monitoring System for High Energy Cosmic Ray Observation in Space Environment using Advanced Electro-optic Pockels Techniques , Conference on Electrical Insulation and Dielectric Phenomena, October 2000
- [3] Y.Zhu, T.Koyama, T.Takada, and Y.Murooka Two-dimensional measurement technique for birefringence vector distribution , Applied Optics, April 1999
- [4] T.Koyama, Y.Zhu, T.Otsuka, T.Takada, and Y.Murooka, An Automatic Measurement System for 2-Dimentional Birefringence Vector conduction and breakdown in solid dielectrics , IEEE, pp.557-560 (1998)